

A model for obesity and gigantism due to disruption of the *Ankrd26* gene

Tapan K. Bera*, Xiu-Fen Liu*, Masanori Yamada*, Oksana Gavrilova†, Eva Mezey‡, Lino Tessarollo§, Miriam Anver¶, Yoonsoo Hahn*||, Byungkook Lee*, and Ira Pastan*.,**

*Laboratory of Molecular Biology, Center for Cancer Research, National Cancer Institute, National Institutes of Health, Bethesda, MD 20892-4264; †Mouse Metabolism Core Laboratory, National Institute of Diabetes, Digestive and Kidney Diseases, National Institutes of Health, Bethesda, MD 20892-0803; ‡Craniofacial and Skeletal Diseases Branch, National Institute of Dental and Craniofacial Research, National Institutes of Health, Bethesda, MD 20892-4479; §Mouse Cancer Genetics Program, Center for Cancer Research, and ¶Pathology/Histotechnology Laboratory, SAIC-Frederick, National Cancer Institute, Frederick, MD 21702

Contributed by Ira Pastan, November 21, 2007 (sent for review October 31, 2007)

Obesity is a major health hazard that is caused by a combination of genetic and behavioral factors. Several models of obesity have been described in mice that have defects in the production of peptide hormones, in the function of cell membrane receptors, or in a transcription factor required for neuronal cell development. We have been investigating the function of a family of genes (*POTE* and *ANKRD26*) that encode proteins that are associated with the inner aspect of the cell membrane and that contain both ankyrin repeats and spectrin helices, motifs known to interact with signaling proteins in the cell. To assess the function of *ANKRD26*, we prepared a mutant mouse with partial inactivation of the *Ankrd26* gene. We find that the homozygous mutant mice develop extreme obesity, insulin resistance, and an increase in body size. The obesity is associated with hyperphagia with no reduction in energy expenditure and activity. The *Ankrd26* protein is expressed in the arcuate and ventromedial nuclei within the hypothalamus and in the ependyma and the circumventricular organs that act as an interface between the peripheral circulation and the brain. In the enlarged hearts of the mutant mice, the levels of both phospho-Akt and mTOR were elevated. These results show that alterations in an unidentified gene can lead to obesity and identify a molecular target for the treatment of obesity.

Akt signaling | coiled-coil motif | insulin resistance | hyperphagia | *POTE* ancestor

We have been studying a family of primate-specific genes termed *POTE*, which are expressed in many cancers and embryonic stem cells, but only in a few normal adult tissues: prostate, ovary, and testis (1–3). The *POTE* genes entered the primate genome ≈ 20 –40 Mya and appear to be under strong selective pressure because they evolved rapidly into 13 closely related paralogs located on 8 different chromosomes (4, 5). They encode proteins that contain three domains: an amino-terminal cysteine-rich domain followed by ankyrin repeats and spectrin-like helices. Different paralogs contain different numbers of each of these components. In addition, an actin retroposon has been inserted in-frame in several family members, indicating that the gene is rapidly evolving in primates (6). The *POTE* genes evolved from a precursor gene, *ANKRD26*, which is located at 10p12.1 in humans and at chromosome 6 (qF1) in the mouse (5). The *ANKRD26* gene also contains ankyrin repeats and spectrin helices but is missing the amino-terminal cysteine-rich domain of *POTE* (5).

EST database analysis of both the human and mouse genomes (www.ncbi.nlm.nih.gov/UniGene/clust.cgi?ORG=Hs&CID=361041) shows that *ANKRD26* RNA is present in many normal tissues, but no function for this gene has been described. To gain information about a possible function for *Ankrd26*, we produced a mutant (MT) mouse in which the *Ankrd26* gene is inactivated by insertion of a β -galactosidase cDNA. We report here that the homozygous *Ankrd26* mutant mice have a very distinct pheno-

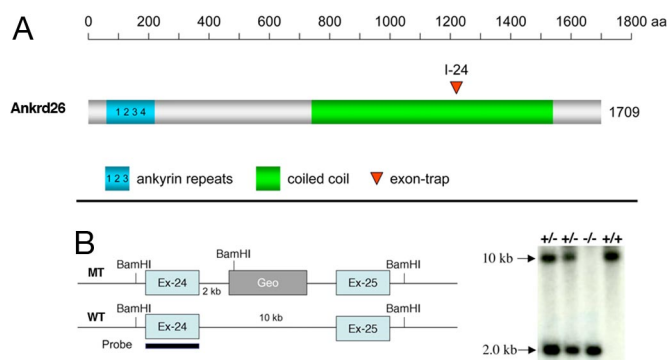


Fig. 1. Schematics showing inactivation of the *Ankrd26* gene. (A) Domain organization of *Ankrd26* protein shown in different colors. Red triangle shows the position of the exon trap mutagenesis of *Ankrd26* protein. (B) Screening strategy and the Southern blot analysis of WT and MT mice. The 10-kb band represents the WT allele; the 2-kb band represents the gene trap-targeted allele.

type consisting of extreme obesity and an increase in organ and body size. The mice also develop insulin resistance.

Results

The mouse *Ankrd26* gene consists of 34 exons spanning a 60-kb region at chromosome band 6qF and is predicted to encode a protein of 192 kDa. To generate a mouse line with inactivation of *Ankrd26*, mouse embryonic stem cells with an insertion of a β -galactosidase gene into the *Ankrd26* locus (Fig. 1) by the gene trap technique were obtained from Bay Genomics (<http://baygenomics.ucsf.edu>) and used to prepare several lines of chimeric mice by conventional techniques. Analysis of the DNA of the mice confirmed that the insertion was located in intron 24 (Fig. 1B). Heterozygous mice were readily obtained, but they had no obvious phenotype. However, we observed that the adult homozygous mice became extremely large and obese as shown in Fig. 2A.

The *Ankrd26* gene is transcribed into a 7.5-kb mRNA and expressed at high level in many tissues, including brain, liver, kidney, heart, as well as in mouse embryos at days 7, 11, 15, and 17 (Fig. 3A). To confirm inactivation of the *Ankrd26* transcript

Author contributions: T.K.B. and I.P. designed research; T.K.B., X.-F.L., M.Y., L.T., and M.A. performed research; L.T. contributed new reagents/analytic tools; T.K.B., O.G., E.M., Y.H., B.L., and I.P. analyzed data; and T.K.B. and I.P. wrote the paper.

The authors declare no conflict of interest.

¶Present address: Department of Life Science, College of Natural Science, Chung-Ang University, Seoul 155-756, Korea.

**To whom correspondence should be addressed at: Laboratory of Molecular Biology, 37 Convent Drive, Room 5106, National Cancer Institute, National Institutes of Health, Bethesda, MD 20892-4264. E-mail: pastani@mail.nih.gov.

Table 1. Metabolic characteristics of 4-month-old *Ankrd26* mutant mice

Characteristic	WT male	Mutant male	WT female	Mutant female
Body weight, g	28.4 ± 1.3	40.1 ± 1.2*	23.2 ± 1.6	40.5 ± 3.1*
Fat mass, g	3.6 ± 0.9	9.5 ± 1.5*	3.5 ± 1.2	16.2 ± 2.4*
Fat mass, % body weight	12.2 ± 2.8	23.2 ± 3.3*	14.1 ± 3.8	39.3 ± 2.9*
Lean mass, g	23.7 ± 0.8	29.1 ± 0.7*	18.3 ± 0.5	22.8 ± 1.1*
Lean mass, % body weight	83.5 ± 2.4	72.9 ± 3.2*	79.8 ± 3.5	57.2 ± 2.7*
Length, mm	83 ± 1.2	91 ± 2	80 ± 1	89 ± 2*
Inguinal fat, g	0.4 ± 0.06	1.0 ± 0.23	0.4 ± 0.2	1.4 ± 0.22*
Gonadal fat, g	0.4 ± 0.08	1.1 ± 0.29	0.6 ± 0.3	2.3 ± 0.35*
Brown fat, g	0.1 ± 0.01	0.2 ± 0.04	0.08 ± 0.02	0.3 ± 0.11
Liver, g	1.5 ± 0.1	2.0 ± 0.20	1.1 ± 0.1	1.6 ± 0.22
Kidney, g	0.4 ± 0.01	0.45 ± 0.20	0.3 ± 0.01	0.33 ± 0.01*
Heart, g	0.15 ± 0.01	0.2 ± 0.02*	0.11 ± 0.01	0.15 ± 0.01*
Serum glucose, mg/dl	243 ± 9	248 ± 29	215 ± 17	281 ± 35
Insulin, ng/ml	0.44 ± 0.05	1.4 ± 0.82	0.34 ± 0.07	0.70 ± 0.11
Triglyceride, mg/dl	79 ± 14	76 ± 20	59 ± 21	75 ± 21
Free fatty acids, mM	0.2 ± 0.04	0.23 ± 0.02	0.35 ± 0.06	0.24 ± 0.03
Leptin, ng/ml	8.8 ± 3.8	25.3 ± 9.8	8.3 ± 4.0	49 ± 16*
Adiponectin, μ g/ml	8.9 ± 0.4	9.7 ± 1.1	17.6 ± 1.8	29.7 ± 5.0

n = 4–5 mice per group. *, *P* < 0.05 versus WT mice of the same sex.

resistance, which is most likely secondary to the obesity phenotype.

To study the mechanism of obesity, we analyzed energy balance in control and MT mice. Both male and female MT mice consumed 4–5 g of food per day, whereas the normal mice consumed \approx 3 g per day (Fig. 4*F*). The difference in food intake was detectable as early as 8 weeks of age (before MT mice became massively obese), suggesting that hyperphagia might be the cause of obesity. Total and resting energy expenditure (per mouse) was significantly higher in MT mice (Fig. 4*G* and *H*). When the data were normalized to lean mass, WT and MT male had a similar metabolic rate, whereas MT females remained hypermetabolic compared with controls (data not shown). Body temperature and activity levels were comparable in control and MT mice (data not shown). Thus, hyperphagia rather than reduction in energy expenditure appear to be the primary cause of obesity in the *Ankrd26* MT mice.

Several lines of obese large mice have been described; the obesity is caused by widespread ectopic expression of the agouti protein (7), mutations in proopiomelanocortin (*POMC*) (8), targeted disruption of the melanocortin-4 receptor (*MC4R*) gene in the brain (9, 10), or haploinsufficiency of *Sim1* gene (11). Using RT-PCR, we analyzed expression of these genes in the hypothalamic region of the brain and found no differences in the RNA level of *POMC1*, agouti-related peptide (*AGRP*), *MC4R*, and *Sim1* between normal and *Ankrd26* MT mice (Fig. 6).

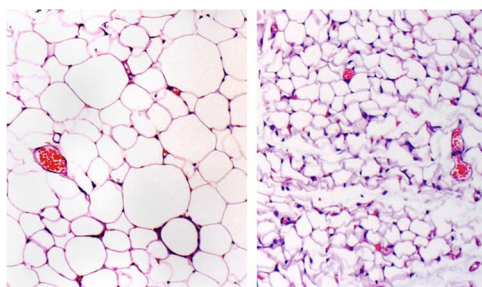


Fig. 5. Histological analysis of mammary fat pad from WT and MT mice. Sections were stained with H&E. (Magnification: \times 10.)

Because the inactivation of the *Ankrd26* is produced by an in-frame insertion of β -galactosidase, one can determine which cells normally produce the *Ankrd26* protein by staining tissue sections with a β -galactosidase substrate (X-Gal). As shown in Fig. 7, *Ankrd26* is expressed in several regions of the brain, which include the arcuate and ventromedial nuclei within the hypothalamus. These nuclei have been shown to have an important role in regulation of feeding behavior (12). The protein is also expressed at high levels in the ependyma and in the circumventricular organs that act as an interface between the peripheral circulation and the brain. Because of the lack of the blood–brain barrier, the sensory circumventricular organs have been suggested to play a central role in the regulation of energy homeostasis (12, 13).

Several proteins and signaling pathways have been implicated in controlling body and organ size and include insulin, insulin receptor (IR), IGF1, IGF1 receptor (IGF1R), IGF2, and the Akt signaling pathway (14, 15). Furthermore, Cantley *et al.* (16) have shown that activation of the Akt pathway in the heart produces

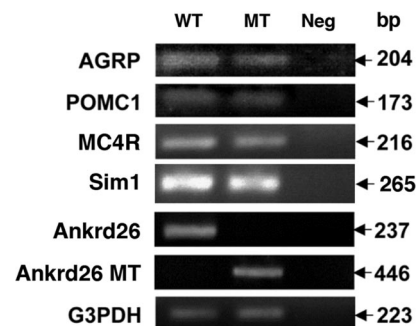


Fig. 6. RT-PCR analysis of RNA from hypothalamus of *Ankrd26* MT and control mouse brain. Expression levels of *AGRP*, *POMC1*, *Sim1*, *MC4R*, *Ankrd26* and *Ankrd26* MT transcripts were measured by RT-PCR using specific primers designed for each gene as described in *Materials and Methods*. For the analysis of the MT *Ankrd26* transcript, the forward primer was within the exon 24 of the *Ankrd26* gene, and the reverse primer was within the *Geo* region of the gene trap vector (<http://baygenomics.ucsf.edu>). Numbers at the right represent the expected size of the amplified product for each gene. *G3PDH* was used as an internal control for the experiment.

large hearts resulting from increased Akt signaling (16). Surprisingly, the phosphorylation of the insulin/IGF1R is also increased in the heart. Although this increase may result from an increase in insulin in the blood, it is modest, and it seems more likely to be caused by some intracellular event controlling receptor phosphorylation such as a decrease in protein phosphatase activity. In liver, where we have observed an increase in fat accumulation in older mice (data not shown), we have also detected an increase in peroxisome proliferator-activated receptor γ (PPAR- γ) mRNA. PPAR- γ has a key regulatory role in adipogenesis and was shown to contribute to hepatic steatosis (23). In addition, the fat cells in lipid depots accumulate large amounts of lipid and continue to produce leptin, indicating that they do not respond to signals regulating the metabolism of lipids. The increase in insulin levels in older mice probably contributes to the accumulation of fat.

A final point of interest is that the human *ANKRD26* gene is located at 10p12, where Price *et al.* (24) have provided information indicating that a gene in this location has a role in some forms of hereditary obesity.

Materials and Methods

Generation of *Ankrd26* MT Mice. *Ankrd26* MT chimeric mice were generated by injection of ES cell line XK525 from Bay Genomics (<http://baygenomics.ucsf.edu>) with methods described in ref. 25. Chimeric males were crossed with C57BL/6 females, and the agouti-colored offspring were analyzed for transmission of the *Ankrd26* mutation. Heterozygous animals were intercrossed to generate homozygous MT animals. WT siblings obtained from the offspring of these crosses were used as control animals in the analysis. All procedures were conducted in accordance with National Institutes of Health guidelines as approved by the Animal Care and Use Committee of the National Cancer Institute and National Institute of Diabetes and Digestive and Kidney Diseases. Mice were typically reared three or four per cage on a 12-h light/dark cycle (lights on 0600–1800) and fed water and NIH-07 diet (11% calories from fat; Zeigler Brothers, Inc.) ad libitum.

Genotyping of MT Mice. Mice were genotyped by Southern blot analysis with DNA extracted from their tails. Genomic DNA was extracted (26), digested with BamHI, run on a 0.9% agarose gel, and blotted onto BioDyne membrane (Life Technology) for Southern blot analysis. The membranes were hybridized with a radiolabeled probe generated by PCR from exon 24 of the *mAnkrd26* sequence. The WT allele gives a band of 10 kb, whereas a band of 2.0 kb represents the correctly targeted allele.

Weight and Length Measurements. Weight gain for individual mice was measured every week with a Sartorius model BL-600 balance beginning at 3–4 weeks of age. Body length of individual mice was measured from nose to anus after immobilization of mice with sedatives.

Food Consumption. Food intake was measured on 8-week-old mice housed in pairs for a period of 2 weeks. A sufficient amount of food was weighed and provided to the mice ad libitum. Each morning, the remaining food was measured, for a total of six measurements. The cages were carefully monitored for evidence of any wastage, which was negligible.

Northern Hybridization. Northern blots containing 2 μ g of poly(A) mRNA from mouse tissues (Clontech) were hybridized with random-primed ³²P-labeled DNA fragments, under high-stringency conditions. Membranes were blocked for >4 h in hybridization solution, hybridized for 15 h with probe at 55°C, rinsed in 2 \times SSC/0.1% SDS, washed twice with 2 \times SSC/0.1% SDS at room temperature, with a final wash at 65°C in 0.2 \times SSC/0.1% SDS.

RT-PCR Analysis. For RT-PCR determination of the expression of various genes, RNA was isolated from hypothalamus of adult mouse brain with TRIzol (Life Technology) reagent. First-strand cDNA was synthesized with a first-strand cDNA synthesis kit (Amersham Biosciences), and PCR was performed with *Taq* polymerase. The PCR conditions used are initial denaturation at 94°C for 1 min, 35 cycles of denaturation at 94°C for 1 min, annealing at 55°C for 1 min, and elongation at 72°C for 1 min. The primers used for PCR amplification of individual genes are as follows: *AGRP*: forward, GGC CTC AAG AAG ACA ACT GC; reverse, GCA AAA GGC ATT GAA GAA GC; *POMC1*: forward, CAT CTT TGT CCC CAG AGA GC; reverse, GCA CCA GCT CCA CAC ATC TA; *MC4R*: forward,

GCT GCA GGA AGA TGA ACT CC; reverse, TCG CCA CGA TCA CTA GAA TG; *Sim1*: forward, CGCTGT GCA CAC CACTTAC; reverse, CCG AGA TAG TGG GAG TGG AA; *Ankrd*: forward, AAG CTG AGA GTC AGC GGC ACA G; reverse, CTC GCG CCT CTT CTA AAT TGC; *Geo*: Reverse, AGT ATC GGC CTC AGG AAG ATC G. For the analysis of the *MT Ankrd26* transcript, the forward primer was within the exon 24 of the *Ankrd26* gene, and the reverse primer was within the *Geo* region of the gene trap vector (<http://baygenomics.ucsf.edu>).

Histological Analysis. WT and *Ankrd26* MT mice were maintained in the same colony following the appropriate animal care and handling guidelines. Mice from each group were euthanized by CO₂ inhalation, and complete necropsies were performed. A comprehensive set of organs and tissues from each animal was fixed in 10% buffered formalin, embedded in paraffin, sectioned at 5 μ m, and stained with H&E. For β -galactosidase staining, the entire brain was frozen in a cryomold with OCT medium. Complex serial/step sections were cut at 10–12 μ m. Serial sections were done through the entire hypothalamus and pituitary. Sequential slides were stained with β -galactosidase and H&E.

Immunofluorescence and Confocal Microscopy. Cells grown on a glass coverslip were washed with PBS and fixed with 4% paraformaldehyde for 30 min. After permeabilization with 0.5% Triton X-100 for 10 min, the samples were then stained with TRITC-labeled phalloidin (Sigma) and DAPI for 5 min. Cells were washed four times with PBS and mounted on glass slides with mounting medium (Invitrogen). All images were obtained with a Zeiss LSM 510 confocal microscope.

Protein Extract and Western Blots. Mice hearts were homogenized in ice-cold lysis buffer [25 mM Tris (pH 7.5), 10 mM EDTA, 10 mM EGTA, 1% Nonidet P-40, 10 μ g/ml leupeptin, 2 μ g/ml aprotinin, 20 μ g/ml PMSF, 100 μ M NaF, 50 μ M NaPP_i, 10 μ M Na₃VO₄]. The lysates were kept on ice for 15 min and then cleared by ultracentrifugation at 150,000 \times g for 20 min. Fifty to 60 μ g of cell extracts were separated by SDS/PAGE. For Western blot analysis, gels were blotted to a PVDF membrane. Blots were sequentially incubated with 5% milk for 1 h in Tris-buffered saline plus 0.1% Triton 100, in primary antibody, anti-P-Akt 473 (1:500), anti-Akt (1:1,000), anti-P-IGF1R (Y1135/1136)/IR (Y1150/1151) (19H7), anti-mTOR, anti-P-mTOR (1:1,000), anti-IR and anti-IGF1R for 1.5 h or overnight, and then in secondary antibody for 1 h. After blotting, signals were detected by ECL (Amersham Biosciences). All primary antibodies were purchased from Cell Signaling Technologies.

Body Composition Analysis. Body composition was measured in nonanesthetized mice with the Echo 3-in-1 NMR analyzer (Echo Medical Systems).

Body Temperature. Body temperature was measured with a rectal probe (model TH-5; Braintree Scientific).

Indirect Calorimetry. Oxygen consumption and carbon dioxide production were measured with a four-chamber Oxymax system (Columbus Instruments) with one mouse per chamber and by testing MT mice simultaneously with littermate controls (27). Motor activity (total and ambulating) was determined by infrared beam interruption (Opto-Varimex mini; Columbus Instruments). Mice had free access to food and water. Total oxygen consumption was measured for 24 h at room temperature (23°C), and energy expenditure was calculated as the average of all points excluding the data from the 1st h of the experiment.

Biochemical Assays. Blood was obtained from the tail vein or retroorbital sinus in the nonfasted state. Blood and serum glucose levels were measured with a Glucometer Elite (Bayer). Serum insulin, leptin, and adiponectin were assayed by RIA (Linco Research). Serum triglycerides (Thermo DMA) and free fatty acid (Roche Applied Science) were measured according to the manufacturers' procedures.

Insulin Tolerance Test. Insulin tolerance tests were performed on nonfasted mice at 8 a.m. Human insulin (Humulin R; Eli Lilly) was injected i.p. (0.75 units/kg). Blood glucose levels were measured 0, 15, 30, 45, 60, 90, and 120 min after the injection.

X-Ray Images. X-ray images were obtained with a Kodak Image Station 4000 multimodal imager with x-ray imaging module (Kodak Molecular Imaging Systems).

Statistical Analysis. Data are expressed as means \pm SE. Statistical significance between the groups was determined with Sigma Stat (SPSS, Inc.), with two-way ANOVA or *t* test as appropriate.

ACKNOWLEDGMENTS. We thank Duc Ha, Jonathan Logue, and Valarmathi Thiruvanamalai for technical assistance; Susan Garfield and Poonam Mannan (Center for Cancer Research Confocal Microscopy Core Facility, National Cancer Institute) for technical support; Dawn Walker for valuable comments; Steve Neal for artwork; and Anna Mazzuca for editorial assistance. This work

was supported in part by the Intramural Research Program of the National Cancer Institute/National Institutes of Health (NCI/NIH), federal funds from NCI/NIH Contract N01-CO12400, the National Institute of Diabetes, Digestive and Kidney Diseases/NIH, and the National Institute of Dental and Craniofacial Research/NIH.

1. Bera TK, Zimonjic DB, Popescu NC, Sathyanarayana BK, Kumar V, Lee BK, Pastan I (2002) *Proc Natl Acad Sci USA* 99:16975–16980.
2. Bera TK, Saint Fleur A, Lee Y, Kydd A, Hahn Y, Popescu NC, Zimonjic DB, Lee B, Pastan I (2006) *Cancer Res* 66:52–56.
3. Bera TK, Saint Fleur A, Ha D, Yamada M, Lee Y, Lee B, Hahn Y, Kaufman DS, Pera M, Pastan I (2008) *Stem Cells Dev*, in press.
4. Bera TK, Huynh N, Maeda H, Sathyanarayana BK, Lee BK, Pastan I (2004) *Gene* 337:45–53.
5. Hahn Y, Bera TK, Pastan IH, Lee BK (2006) *Gene* 366:238–245.
6. Lee Y, Ise T, Ha D, Saint Fleur A, Hahn Y, Liu XF, Nagata S, Lee B, Bera TK, Pastan I (2006) *Proc Natl Acad Sci USA* 103:17885–17890.
7. Bultman SJ, Michaud EJ, Woychik RP (1992) *Cell* 71:1195–1204.
8. Yaswen L, Diehl N, Brennan MB, Hochgeschwender U (1999) *Nat Med* 5:1066–1070.
9. Huszar D, Lynch CA, Fairchild-Huntress V, Dunmore JH, Fang Q, Berkemeier LR, Gu W, Kesterson RA, Boston BA, Cone RD, et al. (1997) *Cell* 88:131–141.
10. Balthasar N, Dalgaard LT, Lee CE, Yu J, Funahashi H, Williams T, Ferreira M, Tang V, McGovern RA, Kenny CD, et al. (2005) *Cell* 123:493–505.
11. Michaud JL, Boucher F, Melnyk A, Gauthier F, Goshu E, Levy E, Mitchell GA, Himms-Hagen J, Fan CM (2001) *Hum Mol Genet* 10:1465–1473.
12. King BM (2006) *Physiol Behav* 87:221–244.
13. Fry M, Hoyda TD, Ferguson AV (2007) *Exp Biol Med* 232:14–26.
14. Conlon I, Raff M (1999) *Cell* 96:235–244.
15. Weinkove D, Leevers SJ (2000) *Curr Opin Genet Dev* 10:75–80.
16. Shioi T, McMullen JR, King PM, Douglas PS, Obata T, Franke TF, Cantley LC, Izumo S (2002) *Mol Cell Biol* 22:2799–2809.
17. Zhang Y, Proenca R, Maffei M, Barone M, Leopold L, Friedman JM (1994) *Nature* 372:425–432, and erratum (1995) 374:479.
18. Chen H, Chariat O, Tartaglia LA, Woolf EA, Weng X, Ellis SJ, Lakey ND, Culpepper J, More KJ, Breitbart RE, et al. (1996) *Cell* 84:491–495.
19. Chua SC, Jr, Chung WK, Wu-peng S, Zhang Y, Liu SM, Tartaglia L, Leibel RL (1995) *Science* 271:994–996.
20. Cool DR, Normant E, Shen F, Chen HC, Pannell L, Zhang Y, Loh YP (1997) *Cell* 88:73–83.
21. Stubdal H, Lynch CA, Moriarty A, Fang Q, Chickering T, Deeds JD, Fairchild-Huntress V, Charlat O, Dunmore JH, Kleyn P, et al. (2000) *Mol Cell Biol* 20:878–882.
22. Yen TY, Gill AM, Frigeri LG, Barsh GS, Wolff GL (1994) *FASEB J* 8:479–488.
23. Gavrilova O, Haluzik M, Matsusue K, Cutson JJ, Johnson L, Dietz KR, Nicol CJ, Vinson C, Gonzalez FJ, Reitman ML (2003) *J Biol Chem* 278:34268–34276.
24. Dong C, Li WD, Geller F, Lei L, Li D, Goriouva OY, Hebebrand J, Amos CI, Nicholls RD, Price RA (2005) *Am J Hum Genet* 76:427–437.
25. Tessarollo L (2001) *Methods Mol Biol* 158:47–63.
26. Laird PW, Zijderveld A, Linders K, Rudnicki MA, Jaenisch R, Berns A (1991) *Nucleic Acids Res* 19:4293.
27. Gavrilova O, Marcus-Samuels B, Reitman ML (2000) *Diabetes* 49:1910–1916.
28. Paxinos G, Franklin KBJ (2001) *The Mouse Brain in Stereotaxic Coordinates* (Elsevier, Amsterdam).